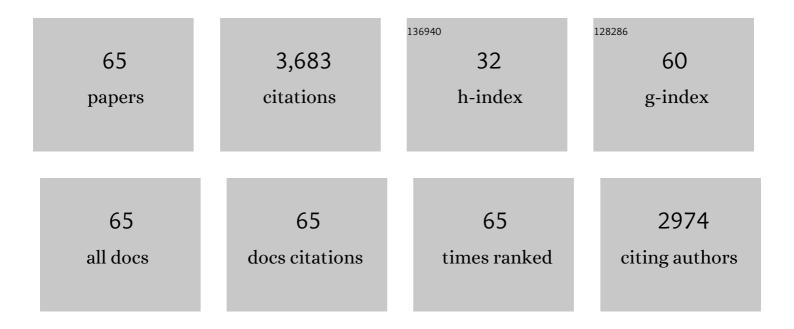
List of Publications by Year in descending order

Source: https://exaly.com/author-pdf/3108906/publications.pdf Version: 2024-02-01



WEI WANG

#	Article	IF	CITATIONS
1	CoFe2O4/N-doped reduced graphene oxide aerogels for high-performance microwave absorption. Chemical Engineering Journal, 2020, 388, 124317.	12.7	312
2	A Dynamic Three-Dimensional Covalent Organic Framework. Journal of the American Chemical Society, 2017, 139, 4995-4998.	13.7	213
3	Synthesis and characterization of gadolinium doped cobalt ferrite nanoparticles with enhanced adsorption capability for Congo Red. Chemical Engineering Journal, 2014, 250, 164-174.	12.7	199
4	3D Nest-Like Architecture of Core–Shell CoFe ₂ O ₄ @1T/2H-MoS ₂ Composites with Tunable Microwave Absorption Performance. ACS Applied Materials & Interfaces, 2020, 12, 11252-11264.	8.0	197
5	PVP-encapsulated CoFe2O4/rGO composites with controllable electromagnetic wave absorption performance. Chemical Engineering Journal, 2019, 373, 755-766.	12.7	173
6	Paramagnetic CoS2@MoS2 core-shell composites coated by reduced graphene oxide as broadband and tunable high-performance microwave absorbers. Chemical Engineering Journal, 2019, 378, 122159.	12.7	168
7	Observation of Interpenetration Isomerism in Covalent Organic Frameworks. Journal of the American Chemical Society, 2018, 140, 6763-6766.	13.7	144
8	Effect of the rare-earth substitution on the structural, magnetic and adsorption properties in cobalt ferrite nanoparticles. Ceramics International, 2016, 42, 4246-4255.	4.8	136
9	Rapid hydrothermal synthesis of magnetic CoxNi1â^'xFe2O4 nanoparticles and their application on removal of Congo red. Chemical Engineering Journal, 2014, 242, 226-233.	12.7	120
10	High-efficiency and selective adsorption of organic pollutants by magnetic CoFe2O4/graphene oxide adsorbents: Experimental and molecular dynamics simulation study. Separation and Purification Technology, 2020, 238, 116400.	7.9	120
11	PEG-assisted hydrothermal synthesis of CoFe2O4 nanoparticles with enhanced selective adsorption properties for different dyes. Applied Surface Science, 2016, 389, 1003-1011.	6.1	116
12	Synthesis, characterization and adsorption capability for Congo red of CoFe2O4 ferrite nanoparticles. Journal of Alloys and Compounds, 2015, 640, 362-370.	5.5	108
13	Constructing multiple heterogeneous interfaces in the composite of bimetallic MOF-derivatives and rGO for excellent microwave absorption performance. Carbon, 2021, 173, 1059-1072.	10.3	107
14	A phytic acid modified CoFe2O4 magnetic adsorbent with controllable morphology, excellent selective adsorption for dyes and ultra-strong adsorption ability for metal ions. Chemical Engineering Journal, 2017, 330, 936-946.	12.7	99
15	3D CoFe2O4 nanorod/flower-like MoS2 nanosheet heterojunctions as recyclable visible light-driven photocatalysts for the degradation of organic dyes. Applied Surface Science, 2018, 447, 711-723.	6.1	92
16	Synthesis and high-efficiency methylene blue adsorption of magnetic PAA/MnFe2O4 nanocomposites. Applied Surface Science, 2015, 346, 348-353.	6.1	89
17	Facile synthesis of rGO/SmFe5O12/CoFe2O4 ternary nanocomposites: Composition control for superior broadband microwave absorption performance. Applied Surface Science, 2018, 453, 464-476.	6.1	85
18	A Three-Dimensional sp ² Carbon-Conjugated Covalent Organic Framework. Journal of the American Chemical Society, 2021, 143, 15562-15566.	13.7	80

#	Article	IF	CITATIONS
19	Microstructure and magnetic properties of MFe2O4 (M = Co, Ni, and Mn) ferrite nanocrystals prepared using colloid mill and hydrothermal method. Journal of Applied Physics, 2015, 117, .	2.5	78
20	Achieving super-broad effective absorption bandwidth with low filler loading for graphene aerogels/raspberry-like CoFe2O4 clusters by N doping. Journal of Colloid and Interface Science, 2021, 590, 186-198.	9.4	77
21	A novel poly(m-phenylenediamine)/reduced graphene oxide/nickel ferrite magnetic adsorbent with excellent removal ability of dyes and Cr(VI). Journal of Alloys and Compounds, 2017, 722, 532-543.	5.5	74
22	3D core-shell Fe3O4@SiO2@MoS2 composites with enhanced microwave absorption performance. Journal of Colloid and Interface Science, 2021, 604, 537-549.	9.4	66
23	Synthesis of nonstoichiometric Co0.8Fe2.2O4/reduced graphene oxide (rGO) nanocomposites and their excellent electromagnetic wave absorption property. Journal of Alloys and Compounds, 2019, 774, 997-1008.	5.5	64
24	Implanting N-doped CQDs into rGO aerogels with diversified applications in microwave absorption and wastewater treatment. Chemical Engineering Journal, 2022, 443, 136475.	12.7	60
25	Anisotropic, multifunctional and lightweight CNTs@CoFe2O4/polyimide aerogels for high efficient electromagnetic wave absorption and thermal insulation. Chemical Engineering Journal, 2022, 442, 136388.	12.7	52
26	Molecular Dynamics Simulation Insight Into Two-Component Solubility Parameters of Graphene and Thermodynamic Compatibility of Graphene and Styrene Butadiene Rubber. Journal of Physical Chemistry C, 2017, 121, 10163-10173.	3.1	51
27	A novel MOF-drived self-decomposition strategy for CoO@N/C-Co/Ni-NiCo2O4 multi-heterostructure composite as high-performance electromagnetic wave absorbing materials. Chemical Engineering Journal, 2021, 426, 131667.	12.7	48
28	3D porous coral-like Co1.29Ni1.71O4 microspheres embedded into reduced graphene oxide aerogels with lightweight and broadband microwave absorption. Journal of Colloid and Interface Science, 2022, 609, 12-22.	9.4	48
29	From nanosphere to nanorod: Tuning morphology, structure and performance of cobalt ferrites via Pr3+ doping. Chemical Engineering Journal, 2016, 306, 382-392.	12.7	43
30	Designing Z-scheme CdS/WS2 heterojunctions with enhanced photocatalytic degradation of organic dyes and photoreduction of Cr (VI): Experiments, DFT calculations and mechanism. Separation and Purification Technology, 2022, 291, 120976.	7.9	41
31	Effect of polyacrylic acid addition on structure, magnetic and adsorption properties of manganese ferrite nanoparticles. Powder Technology, 2016, 295, 59-68.	4.2	37
32	Facile synthesis and high-frequency performance of CoFe2O4 nanocubes with different size. Journal of Magnetism and Magnetic Materials, 2018, 451, 793-798.	2.3	33
33	Achieving effective control of the photocatalytic performance for CoFe2O4/MoS2 heterojunction via exerting external magnetic fields. Materials Letters, 2020, 260, 126979.	2.6	32
34	Hollow Ni/C microsphere@graphene foam with dual-spatial and porous structure on the microwave absorbing performance. Journal of Alloys and Compounds, 2021, 873, 159811.	5.5	32
35	Lightweight and robust cobalt ferrite/carbon nanotubes/waterborne polyurethane hybrid aerogels for efficient microwave absorption and thermal insulation. Journal of Materials Chemistry C, 2021, 9, 12201-12212.	5.5	30
36	PVP modified rGO/CoFe2O4 magnetic adsorbents with a unique sandwich structure and superior adsorption performance for anionic and cationic dyes. Separation and Purification Technology, 2022, 286, 120484.	7.9	27

#	Article	IF	CITATIONS
37	Micro-flower like Core-shell structured ZnCo@C@1T-2H-MoS2 composites for broadband electromagnetic wave absorption and photothermal performance. Journal of Colloid and Interface Science, 2022, 622, 261-271.	9.4	24
38	Current advances of Polyurethane/Graphene composites and its prospects in synthetic leather: A review. European Polymer Journal, 2021, 161, 110837.	5.4	23
39	Topological transformation strategy for layered double hydroxide@carbon nanofibers as highly efficient electromagnetic wave absorber. Journal of Alloys and Compounds, 2021, 867, 159046.	5.5	21
40	Ethanol-assisted synthesis and adsorption property of flake-like NiFe2O4 nanoparticles. Ceramics International, 2015, 41, 13624-13629.	4.8	19
41	Synthesis and Characteristics of Superparamagnetic <scp><scp>Co</scp></scp> _{0.6} <scp><scp>Zn</scp></scp> _{0.4} <scp>Fe</scp> Nanoparticles by a Modified Hydrothermal Method. Journal of the American Ceramic Society, 2013, 96, 2245-2251.	<su< td=""><td>b>2<so 18</so </td></su<>	b>2 <so 18</so
42	Analysis on three-sublattice model of magnetic properties in rare-earth iron garnets under high magnetic fields. Journal of Alloys and Compounds, 2012, 512, 128-131.	5.5	17
43	Study of Mn3O4 doping to improve the magnetic properties of MnZn ferrites. Materials Science and Engineering B: Solid-State Materials for Advanced Technology, 2009, 158, 35-39.	3.5	14
44	Nonreciprocal TE–TM Mode Conversion Based on Photonic Crystal Fiber of Air Holes Filled With Magnetic Fluid Into a Terbium Gallium Garnet Fiber. IEEE Transactions on Magnetics, 2015, 51, 1-4.	2.1	11
45	Development of MnZn ferrites by combinatorial synthesis and high throughput screening method. Journal of Alloys and Compounds, 2008, 463, 112-118.	5.5	10
46	High-Temperature Magnetic Properties of Dysprosium Iron Garnet in Strong Magnetic Fields. IEEE Transactions on Magnetics, 2012, 48, 3638-3640.	2.1	10
47	Mean field analysis of the high temperature magnetic properties of terbium iron garnet in strong DC fields. Journal of Magnetism and Magnetic Materials, 2015, 393, 437-444.	2.3	10
48	Achieving a high cutting-off frequency in the oriented CoFe2O4 nanocubes. Applied Physics Letters, 2017, 111, .	3.3	8
49	Analysis on high-field magnetic properties of aluminum substituted rare-earth iron garnet at low temperatures. Journal of Magnetism and Magnetic Materials, 2014, 360, 193-199.	2.3	6
50	Properties of exchange interaction in Yb3Fe5O12 under extreme conditions. Journal of Magnetism and Magnetic Materials, 2009, 321, 3307-3310.	2.3	5
51	Extension of the molecular-field theory on the magnetic behaviors in paramagnetic Dy3Ga5O12. Journal of Alloys and Compounds, 2009, 488, 23-26.	5.5	5
52	Three-sublattice analyses on magnetic and magneto-optical properties of scandium substituted ytterbium iron garnet in high magnetic fields. Journal of Magnetism and Magnetic Materials, 2015, 374, 333-337.	2.3	5
53	Synthesis and Characterization of Co–Zn Ferrite Nanoparticles by Hydrothermal Method: A Comparative Study. IEEE Transactions on Magnetics, 2015, 51, 1-4.	2.1	5
54	Nonlinear field dependence of the Faraday effect in neodymium gallium garnet under high magnetic field. Physica B: Condensed Matter, 2008, 403, 1-4.	2.7	3

#	Article	IF	CITATIONS
55	High field magnetic anisotropy in praseodymium gallium garnet at low temperatures. Journal of Alloys and Compounds, 2011, 509, 1489-1492.	5.5	3
56	High-field magnetic properties in Nd–Fe intermetallic compound. Journal of Magnetism and Magnetic Materials, 2013, 331, 225-231.	2.3	3
57	Effect of cation size and disorder on the power loss of La0.7(Ba1â^'xSrx)0.3MnO3. Journal of Magnetism and Magnetic Materials, 2010, 322, 1884-1888.	2.3	2
58	Determination of the easy axis of magnetization in terbium–yttrium iron garnet Tb1Y2Fe5O12 at low temperatures. Physica B: Condensed Matter, 2015, 476, 129-131.	2.7	2
59	A general approach to homogeneous sub-nanometer metallic particle/graphene composites by S-coordinator. Solid State Communications, 2018, 273, 17-22.	1.9	2
60	Formation of Samarium Ferrites With Controllable Morphology by Changing the Addition of KOH. IEEE Transactions on Magnetics, 2019, 55, 1-5.	2.1	2
61	Characteristic Features of the Anomalous Magnetic Properties of Some Mixed Terbium–Yttrium Ferrite Garnets at Low Temperatures. IEEE Transactions on Magnetics, 2021, 57, 1-5.	2.1	2
62	Effects of a high DC magnetic field on spin reorientation in dysprosium- yttrium iron garnets at low temperatures. AIP Advances, 2019, 9, 035326.	1.3	1
63	Hydrothermal Synthesis of Various Magnetic Properties of Controlled Micro/Nanostructured Powders and Films of Rare-Earth Iron Garnet. Nanomaterials, 2021, 11, 972.	4.1	1
64	Analysis on an abnormal behavior of magnetization in neodymium trifluoride at low temperatures. Journal of Alloys and Compounds, 2013, 550, 71-74.	5.5	0
65	INDUSTRIAL WASTEWATER PURIFICATION ADSORPTION MATERIALS BASED ON RARE-EARTH FERRITE GARNETS Sm3Fe5O12 Sustainable Development of Mountain Territories, 2021, 13, 629-636	0.3	0